Colloids and Surfaces B: Biointerfaces 122 (2014) 241–249

Contents lists available at ScienceDirect

Colloids and Surfaces B: Biointerfaces

journal homepage: www.elsevier.com/locate/colsurfb

Interfacing Whispering Gallery Mode Optical Microresonator Biosensors with the Plant Defense Elicitor Chitin

Jeremy L. Dahmen[a,1], Yongqiang Yang[b,1], C. Michael Greenlief[c], Gary Stacey[a], Heather K. Hunt[b,*]

[a] Divisions of Plant Sciences and Biochemistry, Christopher S. Bond Life Sciences Center, University of Missouri, Columbia, MO 65211, United States
[b] Department of Bioengineering, Christopher S. Bond Life Sciences Center, University of Missouri, Columbia, MO 65211, United States
[c] Department of Chemistry, Christopher S. Bond Life Sciences Center, University of Missouri, Columbia, MO 65211, United States

ARTICLE INFO

Article history:
Received 27 March 2014
Received in revised form 25 June 2014
Accepted 30 June 2014
Available online 8 July 2014

Keywords:
Chitin
N-acetylchitooligosaccharides
Pathogen-associated molecular patterns
Surface biochemistry
Biosensors

ABSTRACT

The biomaterial class of chitooligosaccharides (chitin), commonly found in insects and fungi, is one of the most abundant on earth. Substantial evidence implicates chitin in mediating a diverse array of plant cellular signaling events, including the induction of plant defense mechanisms against invading pests. However, these recognition and mediation mechanisms, including the binding kinetics between chitin and their plant recognition receptors, are not fully understood. Therefore, the creation of a platform capable of both interfacing with chitin and plant cell receptors, and monitoring their interactions, would significantly advance our understanding of this plant defense elicitor. Recently, a label-free, highly sensitive biosensor platform, based on Whispering Gallery Mode optical microresonators, has been developed to study such biomolecular interactions. Here, we demonstrate how this unique platform can be interfaced with chitin using simple carbohydrate chemistry. The surface chemistry is demonstrated using X-ray photoelectron spectroscopy, fluorescence microscopy, optical profilometry, ellipsometry, and contact angle measurements. The resulting surface is uniform, with an average surface roughness of 1.25 nm, and is active toward chitin recognition elements. Optical loss measurements using standard quantitative cavity analysis techniques demonstrate that the bioconjugated platforms maintain the high performance ($Q > 10^6$) required to track binding interactions in this system. The platform is able to detect lectin, which binds COs, at 10 μg/mL concentration. This biosensor platform's unique capabilities for label-free, high sensitivity biodetection, when properly interfaced with the biomaterials of interest, could provide the basis for a robust analytical technique to probe the binding dynamics of chitin–plant cell receptors.
© 2014 Elsevier B.V. All rights reserved.

1. Introduction

A great number of agriculturally important crops suffer devastating losses every year from plant diseases. Of these diseases, fungal pathogens lead to the largest economic loss [1]. Plants depend upon their innate immune response to defend against these pathogens [2–4]. This immune response is triggered by two levels of microbial recognition: (1) the detection of pathogen (microbe) associated molecular patterns [P(M)AMPs] by pattern recognition receptors (PRRs) and (2) effector triggered immunity (ETI) [3]. PAMPs are characterized both by being structurally conserved, or identical, across a wide array of microbes, and by being not produced by the host. Numerous studies have shown that PAMPs elicit an immune response in a number of agriculturally significant plants, such as soybean, rice, barley, and wheat [5–7]. PAMP signaling is also a key element in animal, including human, innate immunity systems [8,9].

The ability of plants to recognize various PAMPs enables plants to quickly defend against fungal, bacterial, and insect invaders. One of the most common PAMPs is chitin, a fungal cell wall constituent [10]. Chitin is comprised of polymers of N-acetylglucosamine (GlcNAc) residues linked together through a β1–4 glycosidic

Abbreviations: CO(s), chitooligosaccharides; P(M)AMPs, pathogen (microbe) associated molecular patterns; PRRs, pattern recognition receptors; ETI, effector triggered immunity; GlcNAc, N-acetylglucosamine; CEBiP, elicitor binding protein; Os, oryzasativa; CERK1, chitin elicitor receptor kinase 1; MAPK, mitogen-activated protein kinase; ELISA, enzyme-linked immunosorbent assay; WGM, Whispering Gallery Mode; SPR, surface plasmon resonance; APTMS, 3-aminopropyltrimethoxysilane; XPS, X-ray photoelectron spectroscopy; Q factor, quality factor; FITC, fluorescein isothiocyanate.

* Corresponding author at: Department of Bioengineering, Christopher S. Bond Life Sciences Center, 240G, University of Missouri, 1201 East Rollins Street, Columbia, MO 65211, United States. Tel.: +1 573 882 8202.
E-mail address: hunthk@missouri.edu (H.K. Hunt).
[1] These authors contributed equally.

http://dx.doi.org/10.1016/j.colsurfb.2014.06.067
0927-7765/© 2014 Elsevier B.V. All rights reserved.

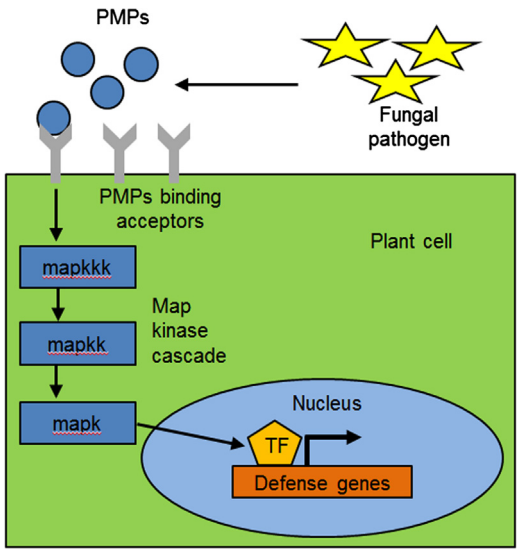

Fig. 1. Model of the PAMP signaling pathway. Fungal pathogens release pathogen-associated molecular patterns (PAMPs), which bind to plant membrane associated pattern recognition receptors. The binding of PAMP leads to activation of the MAPK cascade, ultimately activating transcription factors, which mediate the expression of defense related genes.

Reprinted with permission from Dahmen et al. [20].

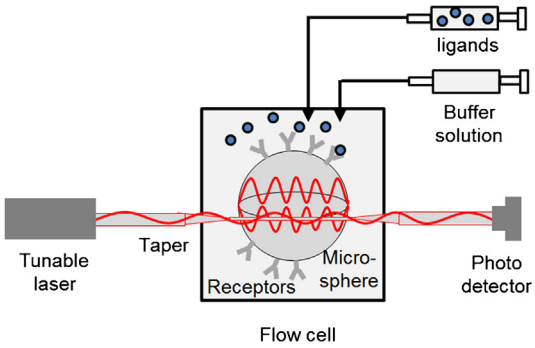

Fig. 2. Schematic of a WGM optical biosensor to detect ligands in buffered solutions. In this WGM optical biosensor platform, the bioconjugated silica microsphere WGM optical microresonator is immersed in a buffer solution within a "micro-aquarium" style housing. Incoming laser light from a tunable laser is coupled into the microsphere by a tapered optical fiber. When analytes are injected into the "micro-aquarium," they are able to bind to the immobilized receptors on the bioconjugated device. This changes the optical properties of the circulating light in the device, leading to detectable shifts in the device's resonant frequency.

linkage. Chitin is synthesized through the action of chitin synthases, which represent a very large gene family, and is found in fungi, insects, bacteria, protozoa, and vertebrates [11]. In order for chitin to induce an immune response in plants, plasma membrane proteins, known as pattern recognition receptors (PRRs), must recognize and bind the chitin (Fig. 1) [12–14].

Several different chitin elicitor binding proteins have been identified in several plant species. Each elicitor has at least one lysine (LysM) domain. For instance, in *Arabidopsis thaliana*, a chitin elicitor receptor kinase (AtCERK1) with three LysM domains and an intracellular serine/threonine kinase domain, has been identified (AtCERK1/LYK1) [15,16]. It is well known that only chitooligosaccharides (COs) of dp > 7 have significant elicitor activity, at least on rice and arabidopsis. However, a key issue with the AtCERK1 structure is its relatively low K_d values, in the μM range, while a variety of biological assays have shown that COs can act at concentrations below 10 nM. Once COs bind to the specific receptors, downstream signaling will occur. Chitin binding to AtCERK1 results in activation of a mitogen-activated protein kinase (MAPK) cascade through phosphorylation (Fig. 1). This signaling cascade is responsible for activating the transcription of genes directly involved in pathogen defense, as well as transcription factors that will activate other defense-related genes (in Fig. 1) [17–19].

Although some aspects of the chitin–receptor systems are reasonably understood, their fundamental interaction processes need to be studied further to elucidate how they trigger immune responses, using a broad range of biological, chemical, and physical approaches [20]. Previous work with label-based affinity binding assays, isothermal titration calorimetry, and molecular methods have established techniques for determining if a plant cell receptor will interact with chitin, but these methods lack either or both the sensitivity or specificity required to further elucidate the kinetic parameters of their actual interactions [20]. An alternative approach, based on a robust, sensitive and specific biosensor, would allow more detailed studies of the kinetic parameters of these interactions, as well as structural data to explain the chitin receptors affinity for various COs.

Optical biosensors are non-destructive sample interrogation methods with an ability to perform extremely sensitive detection in liquid environments due to their high signal-to-noise ratios. Common, high sensitivity optical methods for biosensing include labeled immunoassays, such as the ELISA assays and fluorescent immunoassays. Label-free optical biosensors, such as optical waveguides [21–23], surface plasmon waveguides and resonators [24–29], and WGM microresonators [30], have demonstrated high sensitivity detection in multi-component systems when paired with an appropriate recognition element. These types of highly sensitive optical sensors have easily demonstrated μM to nM thresholds of sensitivity, and in the case of WGM microresonators, shown in Fig. 2, are capable of detection down to the single nanoparticle or single virus level (aM to fM thresholds) [31–34].

The functionality of WGM microresonators as biosensor platforms derives from their high sensitivity to changes in the environment [35]. WGM microresonators can efficiently confine light at specific resonant frequencies, which is then circulated within the microresonator's periphery. Due to their unique geometric optics and inherent signal amplification, WGM microresonators can achieve ultra-low detection limits [33,36–39]. This is because the WGM microresonators' optical field extends slightly into the surrounding environment through evanescence [40,41]. The primary gauge of WGM microresonator performance is the device's quality factor, or Q factor, which describes the photon lifetime (and is dependent on the microresonator's optical loss) in the microresonator and is directly related to its ultimate or ideal sensitivity. For example, a high-Q device ($Q > 1.0E+08$) has a high photon lifetime (>100 ns); a single photon in such a device will circulate, and potentially interact, over 100,000 times [40]. In comparison, planar evanescent sensors, like waveguide sensors or SPR platforms, typically allow input photons to interact only once with the environment. Using high-Q WGM microresonators, the interaction of molecules with the optical field can be detected via shifts in the resonance frequency of the microresonator. This shift is a result of a change in the effective refractive index of the optical field, which itself can be due to small changes in diameter, optical loss, etc. In these devices, the high photon lifetime within the resonator imparts a high degree of sensitivity to the device, enabling the label-free detection of molecules, such as antigens, antibodies, and bacteria [40].

Recently, WGM microresonators have also been used to study the binding kinetics of biomolecular interactions. For example, Soteropulos et al. [42] determined the kinetic parameters of biotin–streptavidin binding using silica microsphere WGM microresonators. For these reasons, this highly sensitive biosensor platform has the potential to be very useful in defining kinetic

parameters for protein–ligand complexes [43–45]. However, for all the platforms mentioned, the primary challenge for tracking binding interactions remains pairing the high sensitivity biosensors with recognition elements that allow the sensor to interface with a specific biologically significant molecule, thereby reducing the risks of false positives and improving the overall device performance in multi-component systems [46–50]. In particular, interfacing semiconductor-type devices with biomolecules such as chitin or chitin receptors represents a significant challenge. Fortunately, there are a few studies on conjugating polymers to inorganic surfaces that could be well-suited to the chitin system [49,51–53]. These early functionalization techniques could be applied to these biosensor platforms, particularly for those platforms, like the WGM microresonators, that are fabricated from silica-based material systems [49,54]. To do this, we must address three primary issues common to translating bioconjugation techniques to 3D devices: (1) biosensor surfaces tend to be easily damaged by typical wet chemistry techniques, resulting in a decrease in device performance; (2) standard protocols for heterogeneous chemistries, such as dispersed particles in solution, must be adapted to microscale devices so that the devices can be evenly functionalized across their 3D surfaces; and (3) plant biochemical reactions and typical bioconjugation strategies must be merged. From a device perspective, any post-fabrication modification that damages the surface, leaves residue on the surface, or results in a non-uniform surface coating, will negatively impact the device performance.

Here, we present a simple method to interface the important fungal cell wall constituent, chitin, to the surface of 3D, silica-based, microspherical, WGM microresonators, enabling the creation of a platform that can interact with identified, plant chitin receptors. This method will greatly expand our ability to probe plant signaling mechanisms via biosensors. Moreover, this report represents the first example of interfacing these types of optical biosensors with plant chemistry, and is the first time that chitin has been successfully, directly, bioconjugated to a functioning sensor surface.

2. Materials and methods

In order to properly interface the biosensor platform with the chitin–chitin receptor system, the chitin must successfully be bioconjugated to the surface. Here, we base our initial approach on early literature describing acid-catalyzed ring-opening reactions, in combination with surface chemistry approaches commonly utilized in on-chip chemical processing [51,55]. Scheme 1 demonstrates the overall approach, which consists of three main steps: (i) surface hydroxylation, (ii) amination, and finally (iii) chitin conjugation via a ring-opening reaction. It is important to note that the chitin used throughout this work is actually a mixture of various COs, due to the high expense of purified octomeric chitin, which is thought to be the primary CO responsible for eliciting defense responses, and that the final addition of the chitin to the surface will yield an attached molecule with one less CO-mer than before, due to the ring-opening reaction. Lastly, we found it essential not to use standard wet chemistry techniques, such as piranha or RCA etches for the hydroxylation step of the syntheses, as this led to a substantial amount of residue and surface damage. Moreover, the number and type of washes at the end of the reaction were required to completely remove any debris from the surface. The primary challenge with these steps was preventing surface damage, which was easily minimized by using a custom-made microsphere holder and reaction vessel.

2.1. Device fabrication

The silica microspheres used in this research were fabricated by gravimetric melting a tip of a stripped, single mode optical fiber (F-SE-OPT, Newport) with a 25 W CO_2 laser (48-2KAM, Synrad) [56]. The microsphere was formed by surface tension during gravimetric melting, resulting in silica microspheres 80–100 μm in diameter with an atomically smooth surface. (For more detailed information on device formation, including protocols and videos, please refer to Soteropulos and Hunt [57].) After fabrication, the microspheres were placed in a microsphere holder and stored in a desiccator until use (see supporting information for microsphere holder description) [57].

2.2. Device bioconjugation

All chemicals and solvents used were certified ACS grade, except as otherwise indicated, and used as received without further purification. In order to successfully bioconjugate the microspheres without damaging the fragile glass surface, which would destroy the underlying device sensitivity during the hydroxylation and amination process, the microspheres were held within the microsphere

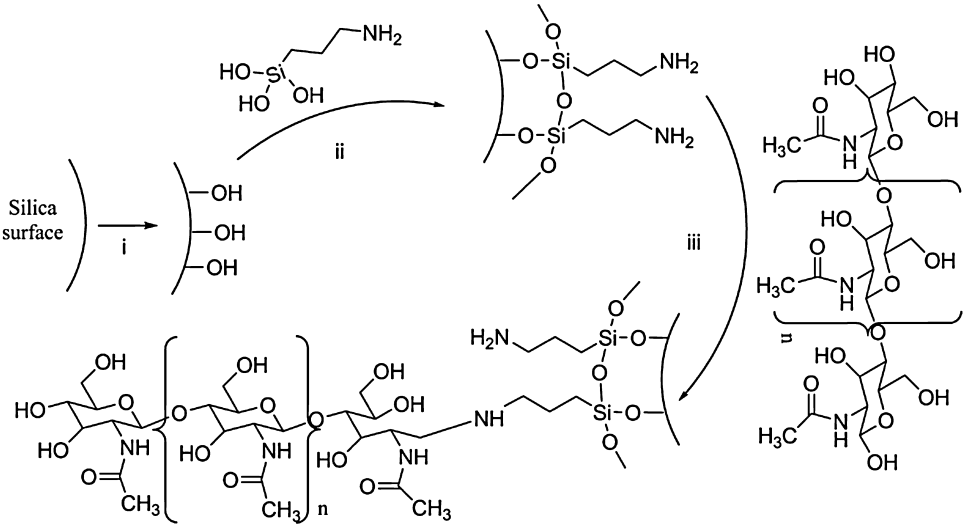

Scheme 1. Three step bioconjugation process to bind COs of various chitin chain lengths to the surface of the silica microspheres. In step (i), the microspheres are subjected to an oxygen plasma etch, creating hydroxyl groups on the silica surface; in step (ii), the hydroxylated microspheres are aminated via a chemical vapor deposition process with a silane coupling agent; and finally, in step (iii), the aminated microspheres are bioconjugated with COs via a ring opening reaction.

Table 1
The reaction conditions of chitin bioconjugation to (1 0 0) Si wafers show that higher temperatures and shorter reaction times produce favorable conjugation results.

Trial	Temperature (°C)	Time (h)	Results
1	50	>50	Poor
2	50	50	Poor
3	50	70	Poor
4	50	<70	Poor
5	80	1	Excellent
6	80	12	Good

holder. The bioconjugation reaction and subsequent washing steps were performed inside a lab-made reaction vessel (see supporting information for microsphere holder and reaction vessel).

First, the silica surface of the microspheres was terminated with hydroxyl groups via an oxygen plasma etch at 200 mTorr pressure, 120 W output power for 5 min (Plasma Cleaner PE-50 Benchtop, Plasma Etch) [58,59]. As demonstrated in the literature, this method of preparing the surface both removes surface contamination and results in surface silanol groups, without damage to the underlying device that more typical wet chemistry procedures, such as piranha or RCA etches, may yield [59].

Second, the hydroxylated microspheres were aminated by grafting silane coupling agents to the silica surface using chemical vapor deposition [59]. Here, the hydroxylated microspheres, stored in the microsphere holder, were exposed to 3-aminopropyltrimethoxysilane (APTMS, Sigma–Aldrich) vapor in a vacuum desiccator under 20 in. Hg vacuum for 15 min [59].

Third, the COs were bound to the aminated microspheres via an acid-catalyzed ring opening reaction (see supplemental information). Sodium cyanoborohydride (Fisher) was used as the reducing agent to open the final ring of the chitin oligomers under an acidic condition by the addition of acetic acid (Aldrich). Here, we used chitin powder (shrimp shells, practical grade, >95%, Sigma–Aldrich), which consists of a variety of CO chain lengths. The chitin powder was suspended in the acidic solution, which was sonicated (Aquasonic 150D, VWR Scientific) for 15 min to improve dispersion. During the reaction with the microspheres, COs were reduced and covalently attached to the aminated silica surface as shown in Scheme 1, using a variety of reaction conditions to discover the optimal conditions that yielded a fully and uniformly bioconjugated surface, without damage to the underlying device (Table 1). For instance, high temperatures and stirring can induce thermal and mechanical stress in the devices, leading to structural damage of the silica surface, device decapitation, and sticky residue that creates areas of non-uniformity. Initial reaction conditions were chosen based on previously reported literature for the ring-opening reaction for chitin [51]. The chitin-bound microspheres were cooled to room temperature and washed with distilled water, methanol (Fisher), acetone (Fisher), heptanes (Aldrich) and acetone (Fisher) for 15 min, in that order, inside a clean reaction vessel on a tilt tray at room temperature. Finally, the microspheres were placed inside the microsphere holder, dried in an 80 °C oven, and then stored in a desiccator.

2.3. Device characterization

Surface characterization of the conjugated devices was performed on both the devices themselves, as well as (1 0 0) silicon wafers (University Wafers), with a thin layer of silica native oxide on the surface, for those techniques that cannot address 3D surfaces. The silicon wafers were cut into 1 cm × 1 cm pieces and then modified by following the same procedures as the microsphere bioconjugation. Surface characterization was done in accordance with literature standards to evaluate surfaces [60].

X-ray photoelectron spectroscopy (XPS) was used to characterize the surface of the bioconjugated silicon wafers at each reaction step. XPS directly probes the surface composition by irradiating the surface of the silica wafers with X-rays (TA-10 twin X-ray source, VSW). The elements on the surface of the silicon wafers can be determined by an electron energy analyzer (15-255GAR, Physical Electronics) from the ejected electrons from the surface of ~10 nm [59].

Fluorescence microscopy (LSM 510 META, Zeiss) was used to confirm the presence of chitin on the silica microsphere surfaces, and to compare reaction conditions in Table 1. Here, we evaluated both the amount of coverage and the quality of that coverage via fluorescent intensity measurements, with the best conditions yielding high intensities that were consistent across several areas of the imaged surface. The chitin-bound microspheres were compared to bare microspheres, to confirm that the fluorescent labeling was successful only on chitin-bound surfaces. Several post-labeling washing steps were done to minimize the possibility of non-specific adsorption of the labeling groups presenting false positives. In each case, the microspheres were incubated in 10 μg/mL lectin$ndash;fluorescein isothiocyanate (lectin–FITC, Sigma–Aldrich) dye in PBS buffer (MP Biomedicals) for 30 min at room temperature. After lectin–FITC conjugation, the microspheres were washed and dried at room temperature. Lectin is a carbohydrate-binding protein that is used as a model for chitin receptors to confirm the availability and activity of the chitin-bioconjugated surface for interaction with proteins and receptors. Lectin is used because the chitin receptors have only recently been identified.

The surface roughness of the conjugated silicon wafers was analyzed by optical profilometry (Wyko NT9100, Veeco). Both bare and bioconjugated silicon wafers were measured to compare the surface roughness before and after bioconjugation, since smooth surfaces are a key element of maintaining the performance of the WGM optical microresonator [61].

Spectroscopic ellipsometry (VB400/HS-190, J. A. Woollam) was used to measure the thickness of the bioconjugated layer on the surface of the silicon wafers. The measurements were performed on both bare silicon wafers and bioconjugated silicon wafers. The reflectance was measured at multiple-angles-of-incidence (65°, 70° and 75°) using a scanning monochromator (HS-190, J. A. Woollam) and a Cauchy model within a wavelength range of 193–3200 nm at multiple points on each wafer. The thickness of the bioconjugated layer was modeled using ellipsometry analysis software (WVASE32, J. A. Woollam), and the resulting thicknesses were compared to optical profilometry data In this case, ellipsometry provides “spot measurements” of the thickness, while optical profilometry provides a wider-range evaluation of surface roughness.

Contact angle measurements (VCA Optima, AST Products) were performed on both silicon bare wafers and bioconjugated silicon wafers. The contact angles were automatically calculated by AutoFAST contact angle calculation software (AST Products).

Although there are many sensing metrics used to judge the performance of a biosensor platform, including the limit of detection, response time, and slope of the response curve, these metrics do not provide as good of an indication of the impact of bioconjugation strategies that add specificity to the device as a direct comparison of the optical loss of the WGM microresonator before and after bioconjugation. Here, a quality factor study was used to analytically characterize the impact of the bioconjugation reactions on the device performance by measuring the resulting changes in optical loss. The optical loss is quantitatively determined by measuring the both the central wavelength of the resonance under investigation, λ, and its full-width at half-maximum, or linewidth, $\Delta\lambda$, and calculating the Q factor ($\lambda/\Delta\lambda$). Here, we measured the Q

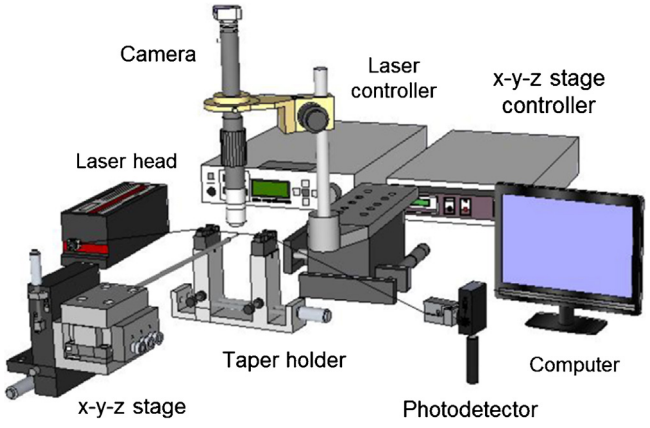

Fig. 3. Schematic of the experimental setup for testing the silica microsphere WGM optical microresonator's performance. Key components are labeled.

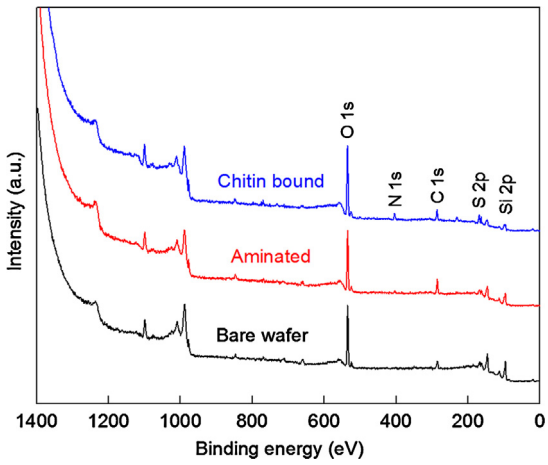

Fig. 4. XPS data. The XPS data show that COs have been successfully biocojugated onto the surface of the silicon wafers, due to the increase in the presence of the nitrogen peak before and after step (iii) in Scheme 1. Peaks of interest are labeled with their corresponding chemical species.

factors of both the as-fabricated (bare, prior to hydroxylation) and chitin-bound microspheres (using only microspheres conjugated using the optimal reaction conditions), and compared these values to determine the impact of the bioconjugation protocols on the device performance. Our key metric for success was to maintain the Q factor above 10^6 post-conjugation, as this has been shown to be the cutoff for performing single virus detection with these devices [62]. In this study, we used standard cavity characterization techniques to evaluate the Q factors of several devices. A tunable, CW, diode laser (TLB6700, Newport), coupled to a tapered optical fiber (F-SE-OPT, Newport), was used to couple ultra-narrow linewidth (~500 kHz) light in the wavelength range of 760–780 nm to the microspheres [63]. As the optical field exited the device, a photodetector (PDA36A, Thorlabs) was used to measure the transmitted optical field (Fig. 3). We did not test the Q factor after reaction steps (i) and (ii) in Scheme 1, as our previous work confirms that these steps do not greatly impact the device sensitivity [44,58,59].

To confirm that the bioconjugated WGM microresonators could then be used in actual detection, detection studies were carried out using 10 μg/mL lectin (from *Triticum vulgaris* (wheat), Aldrich) solution in PBS (MP Biomedicals), injected into a microaquarium directly beneath the microresonator at a flow rate of 0.1 mL/min [42]. As before, a tunable, CW, diode laser (TLB6700, Newport), coupled to a tapered optical fiber (F-SE-OPT, Newport), was used to couple ultra-narrow linewidth (~500 kHz) light in the wavelength range of 760–780 nm to the microspheres [63]. As the optical field exited the device, a photodetector (PDA36A, Thorlabs) was used to measure the transmitted optical field. The WGM microresonator was initially submerged in PBS (MP Biomedicals) and a stable resonance identified. PBS was then injected at a flow rate of 0.1 mL/min, continuing until the injection of the target, also at 0.1 mL/min. Using a custom LabView Sensing Program, the resonance shift upon injection of first the PBS and then the lectin (typically at 50–100 s after the injection of PBS began) was tracked. The sensing program uses GPIB communications, coupled with the provided, prefabricated virtual instruments for the New Focus 6300 series lasers, to monitor the laser's parameters, and to provide sweep mode, step mode, sensogram mode, and a Lorentzian fit mode for combined data collection and analysis. In the sensogram mode, a low-pass Chebyshev 5th order infinite impulse response computational filter (set at 5 MHz) is integrated to reduce background noise for more effective peak tracking. Additionally, the function generator waveform is constantly monitored and the measured slope is used to correct the resonance scan during the sensogram measurement for increased accuracy. Two types of averaging were provided (linear and exponential) to reduce sensogram noise further. In this paper, linear averaging was used at 1 average per time point. Linear averaging combines wavelength measurements together to create a single time point and then moves to the next wavelength measurements to calculate the next time point. This program allows for the accurate, simple, and fast collection of sensograms with low noise and limited post processing.

3. Results and discussion

3.1. Surface chemistry

With the addition of COs, we observed increases in nitrogen and carbon compared to the control wafers in the XPS spectra resulting from several different reaction conditions (Fig. 4). From these data, we determined that the bioconjugation was most successful at 80 °C for 1 h. Other reaction times and temperatures yielded poor results from both a surface chemistry and a device damage perspective. The best reaction conditions were chosen for all future studies, including fluorescence microscopy and device characterization.

Fluorescent micrographs show that, using the best reaction conditions determined via XPS, chitin was successfully and uniformly bound to the aminated silica microspheres (Fig. 5). Analysis of the bioconjugated microspheres showed significant fluorescence compared to the control (bare) microspheres, indicating that the microspheres were successfully bioconjugated with chitin. More importantly, these data showed that the bioconjugation protocols yielded a smooth, uniform surface without damaging the underlying device. This is particularly important, as surface defects, such

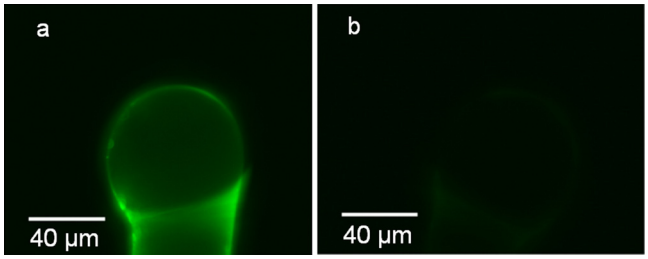

Fig. 5. Fluorescent micrographs of microsphere exposed to lectin-FITC. (a) Bioconjugated microsphere. (b) Bare microsphere. Comparing the bare microsphere (b) to the bioconjugated microsphere (a), it is clear that the bioconjugation successfully yields a uniform surface coverage of chitin that is not the result of physical adsorption.

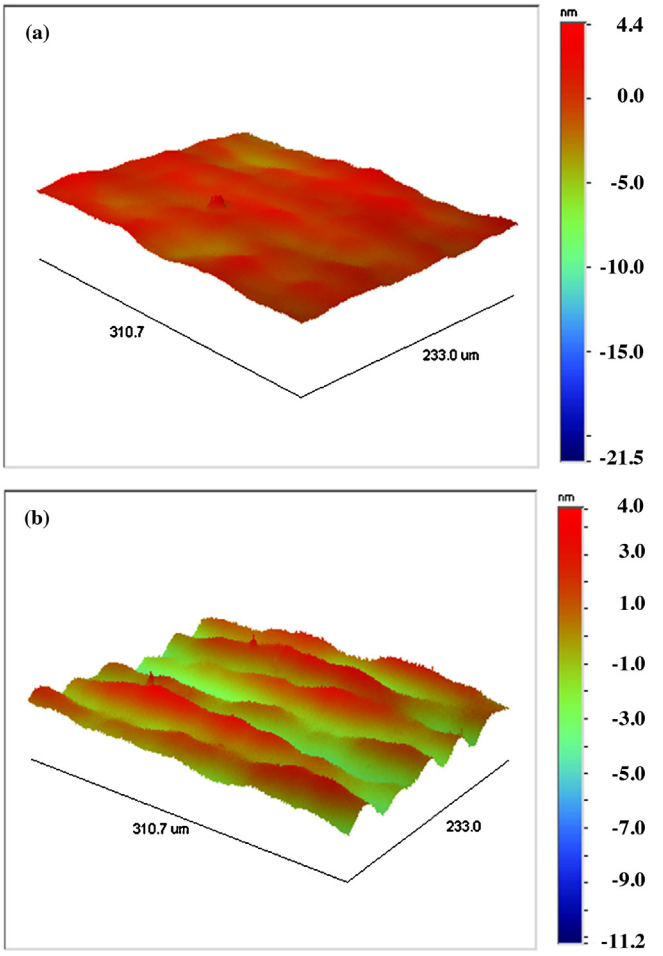

Fig. 6. Optical profilometry measurements for bare wafer (a) and chitin bound wafer (b). The average surface roughness of the bare wafer (a) is 0.79 nm and RMS roughness is 1.05 nm. The average surface roughness of the chitin bound wafer (b) is 1.18 nm and the RMS roughness is 1.48 nm. The overall average is 1.25 nm and σ is 0.28 nm for all the chitin-bound samples examined.

as holes in coverage, debris on the surface, or cracks in the underlying device can increase optical loss, and thus decrease the quality factor and sensitivity of the device [58,64,59]. Lastly, the results indicate that the bioconjugation strategies did not alter the ability of the COs to bind with chitin receptors, like lectin. As previously mentioned, lectin is a good model receptor for chitin, and mimics the actual chitin receptors in plants, which have only recently been discovered.

Optical profilometry test results, shown in Fig. 6, on the chitin-bound silicon wafers showed that the surface of the wafers is relatively uniform. The average surface roughness of the bare wafer (Fig. 6a) is 0.79 nm and RMS roughness is 1.05 nm. The average surface roughness of the chitin bound wafer (Fig. 6b) is 1.18 nm and the RMS roughness is 1.48 nm. The overall average is 1.25 nm and σ is 0.28 nm for all the chitin-bound samples examined. After bioconjugation, the ellipsometry test results on the chitin-bound silicon wafers showed that the chitin layer of the wafer is 9.98 nm (σ, 3.36 nm), which suggests a monolayer of chitin polymers of various lengths was bioconjugated onto a multilayer of organosilanes. At full extension from the surface, the typical chain length of the octomeric CO is ~3.4 nm; when adding the organosilane, we expect a monolayer of each to be ~4 nm in total length. Given that we used a mixture of COs, each of which is a different chain length, we also expect a reasonable amount of variance in both the thickness data from the ellipsometer and the surface roughness data from the optical profilometer, but we would expect that variance to be centered around a mean value of approximately 4 nm, as opposed to 9.98 nm. Given the ring-opening conditions used to bioconjugate the chitin to the surface, it is unlikely that the cause of this higher mean thickness is the result of the COs bonding to each other. It is more likely that the underlying organosilane surface is not a monolayer. Typically, the reaction conditions used yield *at least* a monolayer of organosilanes (as is illustrated in Scheme 1), that form a three-dimensional interconnected network of silane chains extending from the surface [65–68]. This could explain the higher-than-expected thickness at the selected points on the surface. Fortuitously, the fluorescence microscopy data discussed above shows that, regardless of the variance in thickness at various points on the surface, the bioconjugated chitin molecules are still accessible for binding, and maintain their activity. This, combined with the surface uniformity, is the most important aspect of the bioconjugation, since both of these will impact the ability of the device to be used in future sensing studies.

Contact angle measurement showed that the contact angle of the chitin bound silicon wafer was slightly higher than the bare wafer. After bioconjugation, the devices' surfaces still showed hydrophilicity, which is necessary to interact with the chitin receptors in an aqueous environment. The mean of the contact angle (right and left angle) for bare wafer is 67.84° (σ, 0.99°). The mean of contact angle (right and left angle) for chitin bound wafer is 74.15° (σ, 6.99°) (see supporting information for contact angle measurements details).

3.2. Device performance

The as-fabricated (bare) and chitin bioconjugated microspheres were tested to determine the effects of chitin conjugation on the sensitivity of the device at 765–780 nm. This wavelength range was chosen because the absorption of light is lower in water-based solutions (such as serum and buffer) comparing to the longer wavelengths (infrared spectrum) [69]. Therefore, the devices could have a better performance at these wavelengths in future binding kinetics studies. In this case, we required the maintenance of the Q factor above 10^6 after chitin was bioconjugated onto the surface of the microspheres. In Fig. 7, all of the bioconjugated microspheres show Q factors higher than 10^6, although they have slightly lower Q factors than before bioconjugation. In this case, the data suggest that the slightly higher roughness of the coating, as well as the absorption of the chitin molecules themselves in this wavelength regime could account for this reduction in performance. Overall, however, the surface and resonator analysis indicates that this method of interfacing chitin with silica-based devices was successful.

In order to demonstrate that the bioconjugated devices can then be successfully used for actual detection, the chitin bioconjugated microspheres were subjected to a series of detection tests for lectin, the model chitin receptor previously used in conjunction with fluorescence labeling and microscopy to verify that the COs on the surface were still available and active toward binding. As previously mentioned, WGM microresonators rely on the circulating evanescent field, which only exists a short distance from the device surface, to interact with the target of interest. The bioconjugated elements on the surface must be within this field in order for detection to occur as proposed. The ellipsometry data confirms that the surface chemistry is well within the evanescent tail region, and the quantitative cavity analysis confirms that the increase in optical loss caused by the bioconjugation process and the presence of COs on the device will not detrimentally affect sensitivity. In Fig. 8, we show a typical sensor response curve for the detection of lectin, at the same concentration used for the fluorescent studies, with

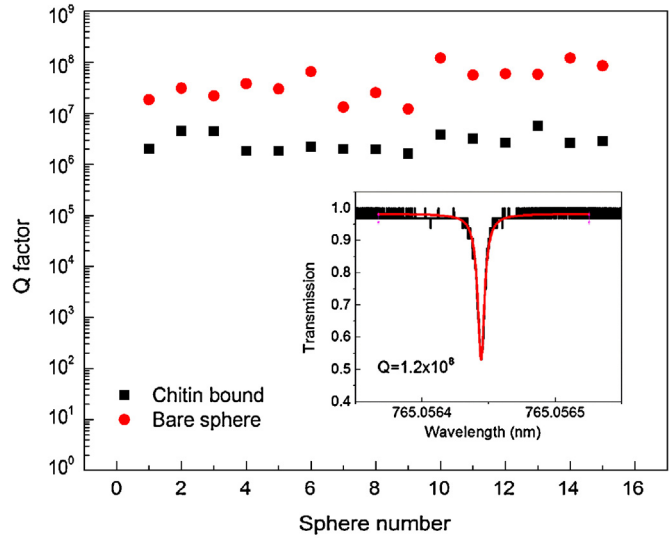

Fig. 7. Quality factors of bare spheres and chitin bound spheres. The mean of Q factors of 15 bare microspheres is 5.1E+07 (σ, 3.6E+07). The mean Q factor after conjugation is 2.9E+06 (σ, 1.2E+06). All functionalized microspheres present a Q factor of above 1.0E+06. Inset: fitting a resonance peak (transmission dip, black) with a Lorentzian (red) to obtain the Q factor for a bare sphere used in this study. (For interpretation of the references to color in this figure caption, the reader is referred to the web version of this article.)

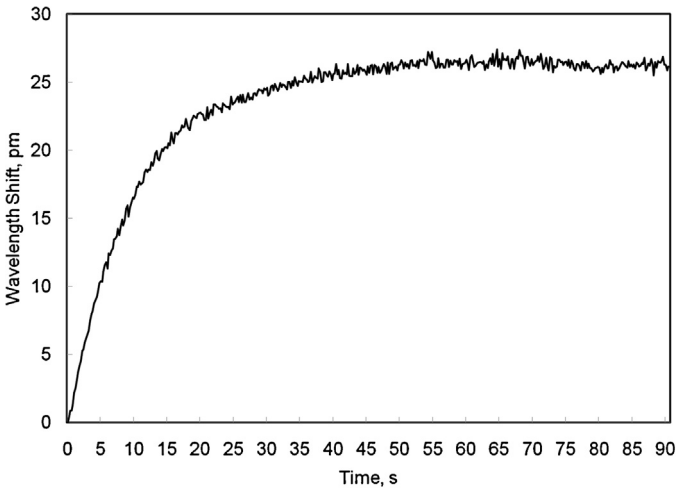

Fig. 8. WGM detection of 10 μg/mL lectin, injected at 0.1 mL/min at time 0, into a PBS-filled microaquarium, in which a chitin-bioconjugated silica microsphere is submerged. The figure shows that the device is capable of performing WGM mode detection.

the bioconjugated microspheres. Fig. 8 shows the beginning of the injection phase to the equilibration phase; prior to this, PBS was injected into the (PBS-filled) microaquarium to confirm that the injection itself does not cause a shift in the resonance wavelength. At the concentration use, a total wavelength shift of 0.020 nm was observed in ~40 s. This confirms that label-free, WGM detection is possible for this interfaced platform, and that there is a good potential that the platform can be used to evaluate chitin–receptor binding interactions at lower concentrations (although it is likely that, for concentrations much above this, the wavelength shift will be too high to track, which places an upper limit on its use).

4. Conclusions

A large number of agriculturally essential crops are negatively impacted every year by fungal plant diseases. A number of studies have shown that COs can elicit an immune response in a number of plants, such as rice, soybean, carrots, barley, tomato, wheat, and Arabidopsis [6,70–73]. Previous studies allowed us to determine the plant cell receptors known to bind chitin. However, we have thus far lacked a technique that can accurately probe the kinetic parameters of these interactions at the appropriate concentration level. Due to their unique capabilities for label-free, high sensitivity and selectivity biodetection, the WGM optical microresonator platform could provide the basis for a robust analytical technique that can probe the binding dynamics of chitin–plant cell receptors. Here, we demonstrate an important first step in this process: identifying the conditions at which such platforms can be successfully bioconjugated to interface with plant systems without negatively impacting the device performance. We confirmed that chitin is conjugated to the microsphere biosensors with a monolayer of COs, without surface or structure damage, and without a significant, negative impact on the high sensitive of the devices. Although previous research has showed that CO derivatives can be spin-coated onto surfaces and then regenerated to a CO monolayer, with a very low roughness values on the surface [55], our method showed high promise in terms of maintaining the overall sensitivity of the biosensor. More significantly, it is suitable to functionalize the surface of the 3D devices, like the microspheres presented here, in addition to planar surfaces, such as the control silica-on-silicon wafers used in the study. Moreover, the bioconjugated COs layer will likely have a higher stability than bioconjugated chitin receptors with regards to storage time, temperature, pH and other environmental changes during fabrication, storage, and detection [48,74,75]. Moreover, the strategies given here can be widely applied to any type of silica-based, 3D structure, allowing many types of devices, beyond this specific biosensor platform, to probe these environments.

Future studies will focus on using these newly developed chitin conjugated biosensors to study receptor–ligand interactions in the CO system. Based on our devices' label-free, high sensitivity and specificity, we can easily detect the bonding behaviors between chitin and its receptors. With these sensing test results, the kinetic parameters of their actual interactions between chitin and their recognition receptors in plants can be further elucidated. Developing a fundamental understanding of how elicitors, such as chitin, interact with plant cell receptors, will provide a more complete picture of plant disease resistance. Broadly speaking, such a detailed picture could lead to the construction of improved, disease-resistant crops, and the ability to help plants perceive and resist a broader range of pathogenic microbes and pests.

Acknowledgements

The authors acknowledge Charissa A. Nowak for the help with ellipsometry, contact angle and profilometry measurements, Mark E. Anderson for the drawing of the schematic of experimental setup for testing microspheres' Q factor, and Benjamin S. Goldschmidt for creating the custom LabView sensing program. The authors also thank the MU International Center for Micro/Nano Systems & Nanotechnology for use of their equipment and expertise. This work was supported by the Division of Chemical Sciences, Geosciences, and Biosciences, Office of Basic Energy Sciences of the U.S. Department of Energy through Grant DE-FG02-08ER15309 to GS.

Appendix A. Supplementary data

Supplementary data associated with this article can be found, in the online version, at http://dx.doi.org/10.1016/j.colsurfb.2014.06.067.

References

[1] A.Y. Rossman, The impact of invasive fungi on agricultural ecosystems in the United States, Biol. Invasions 11 (2009) 97–107.
[2] C. Zipfel, Early molecular events in PAMP-triggered immunity, Curr. Opin. Plant Biol. 12 (2009) 414–420.
[3] T. Boller, S.Y. He, Innate immunity in plants: an arms race between pattern recognition receptors in plants and effectors in microbial pathogens, Science 324 (2009) 742–744.
[4] J.D.G. Jones, J.L. Dangl, The plant immune system, Nature 444 (2006) 323–329.
[5] R.B. Day, M. Okada, Y. Ito, K. Tsukada, H. Zaghouani, N. Shibuya, G. Stacey, Binding site for chitin oligosaccharides in the soybean plasma membrane, Plant Physiol. 126 (2001) 1162–1173.
[6] M. Okada, M. Matsumura, Y. Ito, N. Shibuya, High-affinity binding proteins for N-acetylchitooligosaccharide elicitor in the plasma membranes from wheat, barley and carrot cells: conserved presence and correlation with the responsiveness to the elicitor, Plant Cell Physiol. 43 (2002) 505–512.
[7] N. Shibuya, N. Ebisu, Y. Kamada, H. Kaku, J. Cohn, Y. Ito, Localization and binding characteristics of a high-affinity binding site for N-acetylchitooligosaccharide elicitor in the plasma membrane from suspension-cultured rice cells suggest a role as a receptor for the elicitor signal at the cell surface, Plant Cell Physiol. 37 (1996) 894–898.
[8] S. Akira, K. Takeda, T. Kaisho, Toll-like receptors: critical proteins linking innate and acquired immunity, Nat. Immunol. 2 (2001) 675–680.
[9] T. Nürnberger, F. Brunner, B. Kemmerling, L. Piater, Innate immunity in plants and animals: striking similarities and obvious differences, Immunol. Rev. 198 (2004) 249–266.
[10] M.D. Lenardon, C.A. Munro, N.A.R. Gow, Chitin synthesis and fungal pathogenesis, Curr. Opin. Microbiol. 13 (2010) 416–423.
[11] C.E. Semino, C.A. Specht, A. Raimondi, P.W. Robbins, Homologs of the Xenopus developmental gene DG42 are present in zebrafish and mouse and are involved in the synthesis of Nod-like chitin oligosaccharides during early embryogenesis, Proc. Natl. Acad. Sci. U. S. A. 93 (1996) 4548–4553.
[12] T. Liu, Z. Liu, C. Song, Y. Hu, Z. Han, J. She, F. Fan, J. Wang, C. Jin, J. Chang, J.-M. Zhou, J. Chai, Chitin-induced dimerization activates a plant immune receptor, Science 336 (2012) 1160–1164.
[13] T. Shimizu, T. Nakano, D. Takamizawa, Y. Desaki, N. Ishii-Minami, Y. Nishizawa, E. Minami, K. Okada, H. Yamane, H. Kaku, N. Shibuya, Two LysM receptor molecules, CEBiP and OsCERK1, cooperatively regulate chitin elicitor signaling in rice, Plant J. 64 (2010) 204–214.
[14] L.P. Hamel, N. Beaudoin, Chitooligosaccharide sensing and downstream signaling: contrasted outcomes in pathogenic and beneficial plant–microbe interactions, Planta 232 (2010) 787–806.
[15] A. Miya, P. Albert, T. Shinya, Y. Desaki, K. Ichimura, K. Shirasu, Y. Narusaka, N. Kawakami, H. Kaku, N. Shibuya, CERK1, a LysM receptor kinase, is essential for chitin elicitor signaling in Arabidopsis, Proc. Natl. Acad. Sci. U. S. A. 104 (2007) 19613–19618.
[16] J. Wan, X.-C. Zhang, D. Neece, K.M. Ramonell, S. Clough, S.-Y. Kim, M.G. Stacey, G. Stacey, A LysM receptor-like kinase plays a critical role in chitin signaling and fungal resistance in Arabidopsis, Plant Cell Online 20 (2008) 471–481.
[17] G. Stacey, N. Shibuya, Chitin recognition in rice and legumes, Plant Soil 194 (1997) 161–169.
[18] N. Shibuya, E. Minami, Oligosaccharide signalling for defence responses in plant, Physiol. Mol. Plant Pathol. 59 (2001) 223–233.
[19] X.-C. Zhang, X. Wu, S. Findley, J. Wan, M. Libault, H.T. Nguyen, S.B. Cannon, G. Stacey, Molecular evolution of lysin motif-type receptor-like kinases in plants, Plant Physiol. 144 (2007) 623–636.
[20] J.L. Dahmen, G. Stacey, H.K. Hunt, Current and emerging analytical technologies for analyzing chitin–protein binding interactions, Rev. Anal. Chem. (2013) 1–20.
[21] R. Horvath, H.C. Pedersen, N. Skivesen, D. Selmeczi, N.B. Larsen, Optical waveguide sensor for on-line monitoring of bacteria, Opt. Lett. 28 (2003) 1233–1235.
[22] P. Dumais, C.L. Callender, J.P. Noad, C.J. Ledderhof, Silica-on-silicon optical sensor based on integrated waveguides and microchannels, IEEE Photonic Technol. Lett. 17 (2005) 441–443.
[23] S. Andras, N. Adanyi, I. Szekacs, K. Majer-Baranyi, S. Istvan, Optical waveguide light-mode spectroscopy immunosensors for environmental monitoring, Appl. Opt. 48 (2009) B151–B158.
[24] D.R. Shankaran, K.V.A. Gobi, N. Miura, Recent advancements in surface plasmon resonance immunosensors for detection of small molecules of biomedical, food and environmental interest, Sens. Actuator B: Chem. 121 (2007) 158–177.
[25] F. Sundberg, R. Karlsson, Rapid detection and characterization of immune responses using label-free biacore immunoassays, Immunology 120 (2007) 46–47.
[26] S. Kumbhat, D.R. Shankaran, S.J. Kim, K.V. Gobi, V. Joshi, N. Miura, Surface plasmon resonance biosensor for dopamine using D3 dopamine receptor as a biorecognition molecule, Biosens. Bioelectron. 23 (2007) 421–427.
[27] T. Nagel, E. Ehrentreich-Forster, M. Singh, K. Schmitt, A. Brandenburg, A. Berka, F.F. Bier, Direct detection of tuberculosis infection in blood serum using three optical label-free approaches, Sens. Actuator B: Chem. 129 (2008) 934–940.
[28] K.A. Tetz, L. Pang, Y. Fainman, High-resolution surface plasmon resonance sensor based on linewidth-optimized nanohole array transmittance, Opt. Lett. 31 (2006) 1528–1530.
[29] H.M. Chen, L. Pang, A. Kher, Y. Fainman, Three-dimensional composite metallodielectric nanostructure for enhanced surface plasmon resonance sensing, Appl. Phys. Lett. 94 (2009) 0731171–0731173.
[30] H. Li, X. Fan, Characterization of sensing capability of optofluidic ring resonator biosensors, Appl. Phys. Lett. 97 (2010) 011105.
[31] F. Vollmer, S. Arnold, D. Keng, Single virus detection from the reactive shift of a Whispering Gallery Mode, Proc. Natl. Acad. Sci. U. S. A. 105 (2008) 20701–20704.
[32] F. Vollmer, D. Braun, A. Libchaber, M. Khoshsima, I. Teraoka, S. Arnold, Protein detection by optical shift of a resonant microcavity, Appl. Phys. Lett. 80 (2002) 4057–4059.
[33] N.M. Hanumegowda, I.M. White, H. Oveys, X.D. Fan, Label-free protease sensors based on optical microsphere resonators, Sens. Lett. 3 (2005) 315–319.
[34] J. Zhu, S.K. Ozdemir, Y.-F. Xiao, L. Li, L. He, D.-R. Chen, L. Yang, On-chip single nanoparticle detection and sizing by mode splitting in an ultrahigh-Q microresonator, Nat. Photon. 4 (2010) 122.
[35] I.M. White, N.M. Hanumegowda, X.D. Fan, Subfemtomole detection of small molecules with microsphere sensors, Opt. Lett. 30 (2005) 3189–3191.
[36] M.L. Gorodetsky, A.A. Savchenkov, V.S. Ilchenko, Ultimate Q of optical microsphere resonators, Opt. Lett. 21 (1996) 453–455.
[37] A.B. Matsko, A.A. Savchenkov, D. Strekalov, V.S. Ilchenko, L. Maleki, Review of applications of Whispering-Gallery Mode resonators in photonics and nonlinear optics, in: The Interplanetary Network Progress Report, 42–162, 2005.
[38] N.M. Hanumegowda, C.J. Stica, B.C. Patel, I. White, X.D. Fan, Refractometric sensors based on microsphere resonators, Appl. Phys. Lett. 87 (2005).
[39] I.M. White, H.Y. Zhu, J.D. Suter, N.M. Hanumegowda, H. Oveys, M. Zourob, X.D. Fan, Refractometric sensors for lab-on-a-chip based on optical ring resonators, IEEE Sens. J. 7 (2007) 28–35.
[40] A.M. Armani, R.P. Kulkarni, S.E. Fraser, R.C. Flagan, K.J. Vahala, Label-free, single-molecule detection with optical microcavities, Science 317 (2007) 783–787.
[41] X.D. Fan, I.M. White, S.I. Shopoua, H.Y. Zhu, J.D. Suter, Y.Z. Sun, Sensitive optical biosensors for unlabeled targets: a review, Anal. Chim. Acta 620 (2008) 8–26.
[42] C.E. Soteropulos, H.K. Hunt, A.M. Armani, Determination of binding kinetics using Whispering Gallery Mode microcavities, Appl. Phys. Lett. 99 (2011).
[43] F. Vollmer, S. Arnold, Whispering-Gallery-Mode biosensing: label-free detection down to single molecules, Nat. Meth. 5 (2008) 591–596.
[44] C.E. Soteropulos, H.K. Hunt, A.M. Armani, Determination of binding kinetics using Whispering Gallery Mode microcavities, Appl. Phys. Lett. 99 (2011), 103703–103703-3.
[45] V.S. Ilchenko, A.B. Matsko, Optical resonators with Whispering-Gallery Modes-part II: applications, IEEE J. Sel. Top. Quant. Electron. 12 (2006) 15–32.
[46] D. Erickson, S. Mandal, A.H.J. Yang, B. Cordovez, Nanobiosensors: optofluidic, electrical and mechanical approaches to biomolecular detection at the nanoscale, Microfluid. Nanofluid. 4 (2008) 33–52.
[47] B. Hock, M. Seifert, K. Kramer, Engineering receptors and antibodies for biosensors, Biosens. Bioelectron. 17 (2002) 239–249.
[48] K. Awsiuk, A. Budkowski, P. Petrou, A. Bernasik, M.M. Marzec, S. Kakabakos, J. Rysz, I. Raptis, Model immunoassay on silicon surfaces: vertical and lateral nanostructure vs. protein coverage, Colloid Surf. B: Biointerfaces 103 (2013) 253–260.
[49] S. Guha Thakurta, A. Subramanian, Fabrication of dense, uniform aminosilane monolayers: a platform for protein or ligand immobilization, Colloid Surf. A: Physicochem. Eng. Aspect 414 (2012) 384–392.
[50] J. Hierrezuelo, V. Romero, J. Benavente, R. Rico, J.M. López-Romero, Membrane surface functionalization via theophylline derivative coating and streptavidin immobilization, Colloid Surf. B: Biointerfaces 113 (2014) 176–181.
[51] K. Loos, V. von Braunmühl, R. Stadler, K. Landfester, H.W. Spiess, Saccharide modified silica particles by enzymatic grafting, Macromol. Rapid Commun. 18 (1997) 927–938.
[52] T. Tah, M.T. Bernards, Nonfouling polyampholyte polymer brushes with protein conjugation capacity, Colloid Surf. B: Biointerfaces 93 (2012) 195–201.
[53] S.D. Uzun, N.A. Unlu, M. Sendur, F.E. Kanik, S. Timur, L. Toppare, A novel promising biomolecule immobilization matrix: synthesis of functional benzimidazole containing conducting polymer and its biosensor applications, Colloids Surf. B: Biointerfaces 112 (2013) 74–80.
[54] N. Naveas, J. Hernandez-Montelongo, R. Pulido, V. Torres-Costa, R. Villanueva-Guerrero, J.P. García Ruiz, M. Manso-Silván, Fabrication and characterization of a chemically oxidized-nanostructured porous silicon based biosensor implementing orienting protein A, Colloids Surf. B: Biointerfaces 115 (2014) 310–316.
[55] J.D. Kittle, C. Wang, C. Qian, Y. Zhang, M. Zhang, M. Roman, J.R. Morris, R.B. Moore, A.R. Esker, Ultrathin chitin films for nanocomposites and biosensors, Biomacromolecules 13 (2012) 714–718.
[56] C.E. Soteropulos, K.M. Zurick, M.T. Bernards, H.K. Hunt, Tailoring the protein adsorption properties of Whispering Gallery Mode optical biosensors, Langmuir 28 (2012) 15743–15750.
[57] C.E. Soteropulos, H.K. Hunt, Attaching biological probes to silica optical biosensors using silane coupling agents, J. Vis. Exp. (2012) e3866.
[58] H.K. Hunt, A.M. Armani, Recycling microcavity optical biosensors, Opt. Lett. 36 (2011) 1092–1094.
[59] H.K. Hunt, C. Soteropulos, A.M. Armani, Bioconjugation strategies for microtoroidal optical resonators, Sensors 10 (2010) 9317–9336.
[60] K. Awsiuk, A. Bernasik, M. Kitsara, A. Budkowski, P. Petrou, S. Kakabakos, S. Prauzner-Bechcicki, J. Rysz, I. Raptis, Spectroscopic and microscopic characterization of biosensor surfaces with protein/amino-organosilane/silicon structure, Colloid Surf. B: Biointerfaces 90 (2012) 159–168.
[61] K.J. Vahala, Optical microcavities, Nature 424 (2003) 839–846.

[62] F. Vollmer, S. Arnold, D. Keng, Single virus detection from the reactive shift of a Whispering-Gallery Mode, Proc. Natl. Acad. Sci. U. S. A. 105 (2008) 20701–20704.
[63] J. Knight, G. Cheung, F. Jacques, T. Birks, Phase-matched excitation of Whispering-Gallery-Mode resonances by a fiber taper, Opt. Lett. 22 (1997) 1129–1131.
[64] H.K. Hunt, A.M. Armani, Label-free biological and chemical sensors, Nanoscale 2 (2010) 1544–1559.
[65] R.G. Acres, A.V. Ellis, J. Alvino, C.E. Lenahan, D.A. Khodakov, G.F. Metha, G.G. Andersson, Molecular structure of 3-aminopropyltriethoxysilane layers formed on silanol-terminated silicon surfaces, J. Phys. Chem. C (2012).
[66] N. Aissaoui, L. Bergaoui, J. Landoulsi, J.-F. Lambert, S. Boujday, Silane layers on silicon surfaces: mechanism of interaction, stability, and influence on protein adsorption, Langmuir 28 (2011) 656–665.
[67] B. Arkles, G. Larson, Silicon Compounds: Silanes and Silicones – A Survey of Properties and Chemistry, Gelest, Inc., Morrisville, PA, 2008.
[68] J.B. Brzoska, I. Benazouz, F. Rondelez, Silanization of solid substrates – a step toward reproducibility, Langmuir 10 (1994) 4367–4373.
[69] G.M. Hale, M.R. Querry, Optical constants of water in the 200-nm to 200-μm wavelength region, Appl. Opt. 12 (1973) 555–563.
[70] G. Felix, M. Regenass, T. Boller, Specific perception of subnanomolar concentrations of chitin fragments by tomato cells: induction of extracellular alkalinization, changes in protein phosphorylation, and establishment of a refractory state, Plant J. 4 (1993) 307–316.
[71] N. Shibuya, H. Kaku, K. Kuchitsu, M.J. Maliarik, Identification of a novel high-affinity binding site for N-acetylchitooligosaccharide elicitor in the membrane fraction from suspension-cultured rice cells, FEBS Lett. 329 (1993) 75–78.
[72] B. Zhang, K. Ramonell, S. Somerville, G. Stacey, Characterization of early, chitin-induced gene expression in Arabidopsis, Mol. Plant–Microbe Interact. 15 (2002) 963–970.
[73] Y. Ito, H. Kaku, N. Shibuya, Identification of a high-affinity binding protein for N-acetylchitooligosaccharide elicitor in the plasma membrane of suspension cultured rice cells by affinity labeling, Plant J. 12 (1997) 347–356.
[74] C.A.K. Borrebaeck, Antibodies in diagnostics – from immunoassays to protein chips, Immunol. Today 21 (2000) 379–382.
[75] B. Hock, Antibodies for immunosensors – a review, Anal. Chim. Acta 347 (1997) 177–186.